PERGAMON

Journal of the Mechanics and Physics of Solids
47 (1999) 1113–1130

JOURNAL OF THE
MECHANICS AND
PHYSICS OF SOLIDS

Thermoelastic analysis of periodic thin lines deposited on a substrate

A. Wikström[a], P. Gudmundson[a], S. Suresh[b,*]

[a] *Department of Solid Mechanics, Royal Institute of Technology (KTH), SE-100 44, Stockholm, Sweden*
[b] *Department of Materials and Science and Engineering, Massachusetts Institute of Technology, Cambridge, Massachusetts 02139, U.S.A.*

Received 1 June 1998; accepted 1 September 1998

Abstract

Thermoelastic stresses and curvatures arising from patterned thin lines on initially flat isotropic substrates are analyzed. A connection is made between substrates with patterned lines and laminated anisotropic composites containing transverse matrix cracks. Using this analogy along with anisotropic plate theories, approximate analytical expressions are derived for volume-averaged stresses as well as curvatures along and normal to the lines, for any thickness, width and spacing of the lines. The predictions of the analysis are shown to compare favorably with finite element simulations of stresses and curvatures for Si substrates with Al, Cu or SiO_2 lines. The predictions also match prior experimental measurements of curvatures along and normal to patterned SiO_2 lines on Si wafers, and further capture the general experimental trends reported previously for curvature evolutions in Si wafers with Al lines. The model presented here thus provides a very convenient and simple analytical tool for extracting stresses in thin lines on substrates from a knowledge of experimentally determined film stress, thereby circumventing the need for detailed computations for a wide range of unpassivated line geometries of interest in microelectronic applications. © 1999 Elsevier Science Ltd. All rights reserved.

Keywords: A. Thermomechanical processes; B. Constitutive behavior principles; Thermal stress; Plates; Residual stress

1. Introduction

Discontinuous and periodic lines, which are etched or patterned into different periodic geometrical forms on thick substrates, are commonly encountered in a variety

* Corresponding author. Tel.: 001 617 253 3320; fax: 001 617 253 0868; e-mail: ssuresh@mit.edu

0022–5096/99/$ - see front matter © 1999 Elsevier Science Ltd. All rights reserved
PII: S0022–5096(98)00092–1

of practical situations. A widely known example is one of metal conduction lines patterned onto various substrates and interlayers in microelectronic devices and components.

The reliability of microelectronic devices is strongly influenced by the internal stresses which develop in the interconnect structures. Sources of such stresses include: (a) thermal expansion/contraction mismatch between dissimilar materials, such as the interconnect, dielectric and passivation layers, caused by temperature excursions introduced during processing, manufacture and service, (b) non-equilibrium conditions introduced during the deposition of a continuous film on a substrate, (c) various mechanical processes used to create geometrical and topological changes during etching and patterning of interconnect lines and during planarization, (d) diffusion and chemical reactions which occur at and across interfaces during thermal excursions, (e) the passage of electric current in the conduction lines which introduces nonuniform atomic transport and (f) the absorption of substances such as water vapor.

The estimation of stresses in thin continuous films on substrates is commonly achieved by recourse to the Stoney (1909) analysis. Here the uniform stress in the film is related to the experimentally measured change in curvature of the film/substrate system, from some reference stress-free state. An appealing feature of the Stoney formula is that the thin film stress can be estimated directly from the curvature measurements using only the properties of the substrate material and the geometry of the film and the substrate. This approach does not require a knowledge of the properties of the thin film.

The evolution of curvatures and stresses in patterned lines on deformable substrates is a significantly more complex problem. Aleck (1949), and Blech and Levi (1981) discussed semi-analytical methods for the determination of non-uniform elastic stress distributions within patterned lines on substrates. Their method idealized the cross section of a line as an isolated rectangular plate clamped on a rigid substrate. By treating the finite-sized thin line as a membrane and the substrate as a half plane, Blech and Meieran (1967), Hu (1979) and Isomae (1981) solved for the stresses in the substrate in the vicinity of a film or line edge. Analytical and semi-analytical formulations for the deformation of unpassivated or passivated lines on substrates have also been attempted by Korhonen et al. (1991), Moske et al. (1993) and Yeo et al. (1995). In these analyses, the evolution of stresses and curvatures in etched lines of arbitrary geometry cannot be extracted from a knowledge of the stress in the continuous film, from which they are etched.

The finite element (FE) method provides a means for the estimation of curvature as well as stress distributions in the lines and the substrate. Finite element simulations of stresses in passivated and unpassivated lines have been compared with X-ray measurements (e.g. Jones and Basehore, 1987; Sauter and Nix, 1992; Yeo et al., 1995; Besser et al., 1996). Generalized plane strain formulations within the context of finite element analyses have also been used to predict curvature evolution along and across elastic or elastoplastic lines on elastic substrates for direct comparisons with wafer curvature measurements (Shen et al., 1996; Gouldstone et al., 1998). While these numerical methods estimate stress distributions and curvature evolution in complex

line geometries, they do not offer simple and general theoretical capabilities by recourse to which the deformation of lines on substrates can be conveniently captured.

The objective of the present work was to develop a comprehensive thermoelastic theory for the estimation of average stresses and curvatures in patterned thin lines on thick substrates. A goal of this work was to develop analytical expressions with which the development of stresses and curvatures along and normal to the lines could be predicted from a knowledge of the uniform initial stress or initial curvature in a continuous thin film from which the periodic lines of arbitrary thickness, width and spacing are patterned. These analytical results would also lead to the simplification that different components of stresses in the lines could be estimated from the experimentally determined curvatures along and across the lines. The predictions of this analysis are compared with finite element simulations as well as available experimental results for several different line/substrate systems of practical interest in microelectronics.

2. Thermoelastic model

The geometry of the line/substrate system considered here is defined in Fig. 1. It will subsequently be assumed that the thickness of the lines (t) is much smaller than the substrate thickness (h), with the nondimensional quantity $\delta = t/h \ll 1$. In many practical applications, such as in microelectronic devices, the in-plane dimensions of substrates (i.e. Si wafers) as well as the radii of curvatures are much larger than the cross-sectional dimensions of the lines. This makes it possible to treat the substrate with deposited lines as a homogenized anisotropic plate.

2.1. Plate theory notations

If standard plate theory notation is used, the constitutive relation for the homogenized plate may be written in matrix form as:

$$\begin{bmatrix} \boldsymbol{N} \\ \boldsymbol{M} \end{bmatrix} = \begin{bmatrix} \boldsymbol{A} & \boldsymbol{B} \\ \boldsymbol{B} & \boldsymbol{D} \end{bmatrix} \left(\begin{bmatrix} \boldsymbol{\varepsilon} \\ \boldsymbol{\kappa} \end{bmatrix} - \begin{bmatrix} \boldsymbol{\alpha} \\ \boldsymbol{\beta} \end{bmatrix} \Delta T \right), \tag{1}$$

where

$$\boldsymbol{N} = \begin{bmatrix} N_{11} \\ N_{22} \\ N_{12} \end{bmatrix}, \quad \boldsymbol{M} = \begin{bmatrix} M_{11} \\ M_{22} \\ M_{12} \end{bmatrix}, \quad \boldsymbol{\varepsilon} = \begin{bmatrix} \varepsilon_{11} \\ \varepsilon_{22} \\ 2\varepsilon_{12} \end{bmatrix}, \quad \boldsymbol{\kappa} = \begin{bmatrix} \kappa_{11} \\ \kappa_{22} \\ 2\kappa_{12} \end{bmatrix}, \quad \boldsymbol{\alpha} = \begin{bmatrix} \alpha_{11} \\ \alpha_{22} \\ 2\alpha_{12} \end{bmatrix}, \quad \boldsymbol{\beta} = \begin{bmatrix} \beta_{11} \\ \beta_{22} \\ 2\beta_{12} \end{bmatrix}, \tag{2}$$

and $\boldsymbol{N}$ and $\boldsymbol{M}$ denote membrane forces and moments per unit length, respectively; $\boldsymbol{\varepsilon}$ and $\boldsymbol{\kappa}$ are substrate mid-plane strains and curvatures, respectively; $\boldsymbol{\alpha}$ and $\boldsymbol{\beta}$ are substrate mid-plane coefficients of thermal expansion and thermal curvature, respectively; $\boldsymbol{A}$, $\boldsymbol{B}$ and $\boldsymbol{D}$ are 3×3 symmetric stiffness matrices and ΔT, the temperature change.

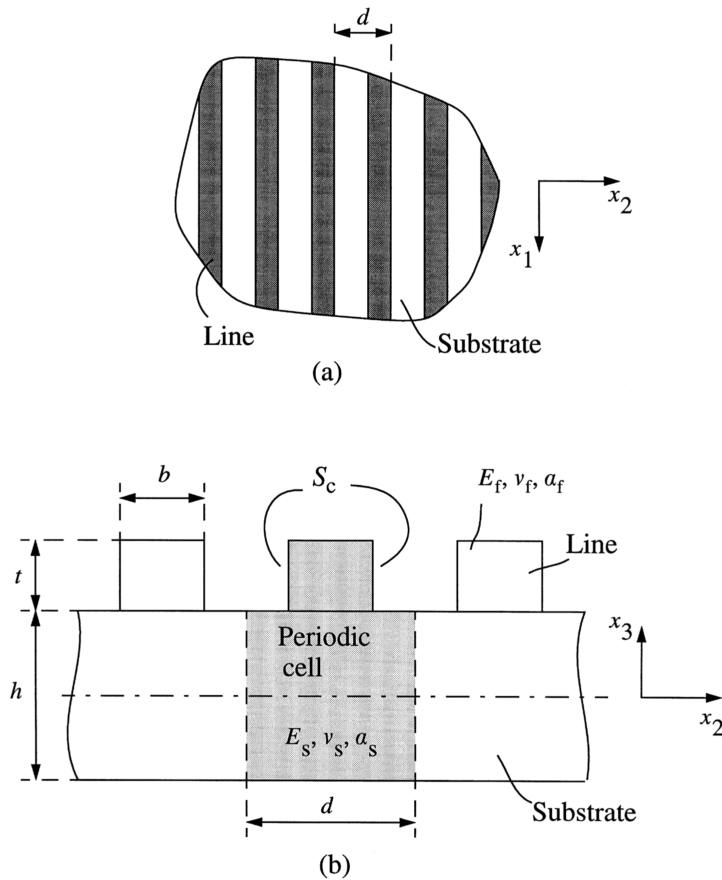

Fig. 1. (a) Top and (b) in-plane view of the periodic line geometry on the substrate.

For an initially stress-free flat plate of arbitrary in-plane shape with free edges, the curvatures and middle surface strains due to uniform heating are given by:

$$\boldsymbol{\varepsilon} = \boldsymbol{\alpha}\Delta T, \quad \boldsymbol{\kappa} = \boldsymbol{\beta}\Delta T. \tag{3}$$

These expressions can be integrated to obtain expressions for the displacements. Hence, the important parameters for an initially flat substrate-line system with free edges are $\boldsymbol{\alpha}$ and $\boldsymbol{\beta}$. Since the line thickness is assumed to be much smaller than the substrate thickness ($\delta \ll 1$), the homogenized thermal expansion coefficients $\boldsymbol{\alpha}$ are almost the same as the thermal expansion coefficient of the bare substrate. The coefficients of thermal curvature $\boldsymbol{\beta}$ does, however, change from zero to a nonzero value due to the effect of the lines on the bare substrate.

2.2. Theoretical formulation

In this section, approximate analytical models for the thermal expansion vector and volume-averaged stresses in the lines are derived. Begin with the total strain energy per unit area (w) in a plate which generally can be written as

$$w = \frac{1}{2}(\boldsymbol{e} - \boldsymbol{a}\Delta T)^T \boldsymbol{C}(\boldsymbol{e} - \boldsymbol{a}\Delta T) + f(\Delta T), \tag{4}$$

where the strain vector, thermal expansion vector and stiffness matrix are defined, respectively, as

$$\boldsymbol{e} = \begin{bmatrix} \boldsymbol{\varepsilon} \\ \boldsymbol{\kappa} \end{bmatrix}, \quad \boldsymbol{a} = \begin{bmatrix} \boldsymbol{\alpha} \\ \boldsymbol{\beta} \end{bmatrix}, \quad \boldsymbol{C} = \begin{bmatrix} \boldsymbol{A} & \boldsymbol{B} \\ \boldsymbol{B} & \boldsymbol{D} \end{bmatrix} \tag{5}$$

and $f(\Delta T)$ is the elastic energy from pre-existing residual stresses which may arise from such factors as non-equilibrium cooling, phase transformations, shrinkage mismatch or epitaxial strain.

The generalized stresses can now be obtained from

$$\boldsymbol{\sigma} = \frac{\partial w}{\partial \boldsymbol{e}} = \boldsymbol{C}(\boldsymbol{e} - \boldsymbol{a}\Delta T) \tag{6}$$

where

$$\boldsymbol{\sigma} = \begin{bmatrix} \boldsymbol{N} \\ \boldsymbol{M} \end{bmatrix} \tag{7}$$

gives mid-surface forces and moments per unit length at the mid-plane of the substrate. If a general expression for w can be found, then $\boldsymbol{C}$ and $\boldsymbol{a}$ can be identified.

Thermoelastic loads are defined by prescribing the effective strains $\boldsymbol{e}$ and the temperature change ΔT on the geometry in Fig. 1. An attempt is now made to determine w. The resulting displacements u_i and stresses σ_{ij} in the body are written as

$$u_i = u_i^0 + u_i'$$
$$\sigma_{ij} = \sigma_{ij}^0 + \sigma_{ij}' \tag{8}$$

where the Latin indices, i, j, take the values 1–3 and the summation convention is utilized. Let the displacements u_i^0 and stresses σ_{ij}^0 represent the well known solution of a thin continuous film subjected to the loads $\boldsymbol{e}$ and ΔT. The displacements u_i' must therefore satisfy the condition that $\boldsymbol{e} = \boldsymbol{0}$. Denoting the free side walls of the lines as S_c (Fig. 1), the boundary conditions on S_c can be expressed as

$$T_i^0 + T_i' = 0 \tag{9}$$

where T_i^0 is the surface traction vector that originates from the 'thin film problem' and T_i' is the surface traction required to impose free sidewalls of the lines. The surface traction vectors may be expressed in terms of stresses as $T_i = \sigma_{ij} n_j$ where n_j denotes

the normal vector of the surface. By denoting the strain and stress corresponding to u_i' as ε_{ij}' and σ_{ij}', respectively, the total strain energy for a periodic element is expressed as:

$$W = \frac{1}{2}\int_V \sigma_{ij}(\varepsilon_{ij} - \alpha_{ij}\Delta T)\,\mathrm{d}V = \frac{1}{2}\int_V (\sigma_{ij}^0 + \sigma_{ij}')(\varepsilon_{ij}^0 - \alpha_{ij}\Delta T + \varepsilon_{ij}')\,\mathrm{d}V \tag{10}$$

where V is the volume of the periodic element, ε_{ij} the strain tensor and α_{ij} the tensor of thermal expansion coefficients. This expression, in expanded form, becomes

$$W = \frac{1}{2}\int_V \{\sigma_{ij}^0(\varepsilon_{ij}^0 - \alpha_{ij}\Delta T) + \sigma_{ij}^0\varepsilon_{ij}' + \sigma_{ij}'(\varepsilon_{ij}^0 - \alpha_{ij}\Delta T) + \sigma_{ij}'\varepsilon_{ij}'\}\,\mathrm{d}V. \tag{11}$$

It can be shown that due to reciprocity, the second and third terms in eqn (11) are equal, such that

$$W = \frac{1}{2}\int_V \{\sigma_{ij}^0(\varepsilon_{ij}^0 - \alpha_{ij}\Delta T) + 2\sigma_{ij}^0\varepsilon_{ij}' + \sigma_{ij}'\varepsilon_{ij}'\}\,\mathrm{d}V. \tag{12}$$

The second term in eqn (12) is now investigated separately:

$$\int_V \sigma_{ij}^0\varepsilon_{ij}'\,\mathrm{d}V = \int_S T_i^0 u_i'\,\mathrm{d}S = \int_{S-S_\mathrm{c}} T_i^0 u_i'\,\mathrm{d}S - \int_{S_\mathrm{c}} T_i' u_i'\,\mathrm{d}S. \tag{13}$$

where S is the surface of the unit cell. It is noted that due to periodicity

$$\int_{S-S_\mathrm{c}} T_i^0 u_i'\,\mathrm{d}S = 0 \tag{14}$$

since on this surface, either $T_i^0 = 0$ on the top and bottom surface, or the contribution from the left edge exactly cancels the contribution from the right edge. By the same argument it can be shown that

$$\int_V \sigma_{ij}'\varepsilon_{ij}'\,\mathrm{d}V = \int_S T_i' u_i'\,\mathrm{d}S = \int_{S_\mathrm{c}} T_i' u_i'\,\mathrm{d}S \tag{15}$$

and hence the total strain energy may be written as

$$W = \frac{1}{2}\int_V \sigma_{ij}^0(\varepsilon_{ij}^0 - \alpha_{ij}\Delta T)\,\mathrm{d}V - \frac{1}{2}\int_{S_\mathrm{c}} T_i' u_i'\,\mathrm{d}S. \tag{16}$$

Expressing the volume of the unit cell V as $V = V_0 - \Delta V$, where V_0 is the volume of the unit cell with a continuous film of thickness t, eqn (16) takes the form

$$W = \frac{1}{2}\int_{V_0} \sigma_{ij}^0(\varepsilon_{ij}^0 - \alpha_{ij}\Delta T)\,\mathrm{d}V - \frac{1}{2}\int_{\Delta V} \sigma_{ij}^0(\varepsilon_{ij}^0 - \alpha_{ij}\Delta T)\,\mathrm{d}V - \frac{1}{2}\int_{S_\mathrm{c}} T_i' u_i'\,\mathrm{d}S. \tag{17}$$

The first two integrals in eqn (17) may be expressed in terms of the solution to the thin film problem. In order to proceed, an approximation to the third integral must

be derived. This term corresponds to the work done by the tractions T_i' on the surface S_c.

2.3. Analogy with anisotropic plates with surface cracks

In order to estimate this last term on the right hand side of eqn (17), it is appropriate at this point to draw an analogy between the geometry of patterned lines on substrates (Fig. 1) and anisotropic plates with surface cracks (Fig. 2). If the thermoelastic properties of a substrate with a cracked surface layer are considered, the strain energy may be expressed by eqn (17) with $\Delta V = 0$. The third integral in eqn (17) would in this case be the work done by the tractions T_i' on the crack surfaces. Accurate expressions for this work have been determined by Gudmundson and Zang (1993). It is now assumed that the work on S_c can be approximated by the crack surface work even when $\Delta V \neq 0$. With this assumption, it is possible to derive approximate analytical expressions for the thermoelastic response of patterned lines on substrates, Fig. 1.

According to Gudmundson and Zang (1993), the last term in eqn (17) can be written as

$$W' = -\frac{1}{2}\int_{S_c} T_i' u_i' \,\mathrm{d}S = -\frac{1}{2} t^2 l \boldsymbol{\tau}^{\mathrm{T}} \Pi \boldsymbol{\tau} \tag{18}$$

where l is the length of the volume V_0 along the lines, $\boldsymbol{\tau}$ the crack surface traction resulting from the thin film solution, and Π, a diagonal 3×3 matrix computed by Gudmundson and Zang (1993) that relates average crack opening displacement per unit crack length to surface tractions. The elastic energy per unit area of the unit cell can then be written as

$$w' = W' \frac{1}{ld} = -\frac{1}{2} t \left(\frac{b}{d}\right) \rho \boldsymbol{\tau}^{\mathrm{T}} \Pi \boldsymbol{\tau} \tag{19}$$

where the line aspect ratio $\rho = t/b$ has been introduced. Here, the only contribution

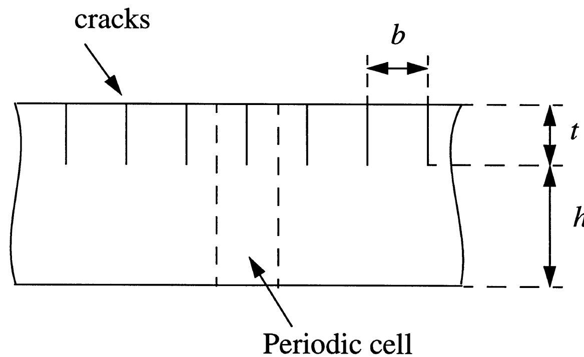

Fig. 2. Substrate with a cracked surface layer, as an analogue for the line-substrate system.

to w' comes from σ_{22}, which is the stress in the thin film without cracks. This stress is expressed in terms of middle surface strains and curvatures by the relation

$$\sigma_{22} = \boldsymbol{Q}_{\mathrm{f}}(\boldsymbol{e} - \boldsymbol{a}_{\mathrm{f}}\Delta T) \tag{20}$$

where

$$\boldsymbol{Q}_{\mathrm{f}} = \frac{E_{\mathrm{f}}}{1-v_{\mathrm{f}}^2}\left[v_{\mathrm{f}} \quad 1 \quad 0 \quad v_{\mathrm{f}} \quad \frac{h}{2} \quad \frac{h}{2} \quad 0\right], \quad \boldsymbol{a}_{\mathrm{f}}^T = [a_{\mathrm{f}} \quad a_{\mathrm{f}} \quad 0 \quad 0 \quad 0 \quad 0] \tag{21}$$

and E_{f} and v_{f} are Young's modulus and Poisson ratio, respectively, of a continuous film made of the same material as the lines. The energy per unit area w' can now be expressed as

$$w' = -\frac{1}{2}t\left(\frac{b}{d}\right)\rho\Pi_{22}(\boldsymbol{e} - \boldsymbol{a}_{\mathrm{f}}\Delta T)^{\mathrm{T}}\boldsymbol{Q}_{\mathrm{f}}^{\mathrm{T}}\boldsymbol{Q}_{\mathrm{f}}(\boldsymbol{e} - \boldsymbol{a}_{\mathrm{f}}\Delta T) \tag{22}$$

where the quantity Π_{22} has been computed by Gudmundson and Zang (1993). The function

$$\chi(\rho) = \frac{E_{\mathrm{f}}}{1-v_{\mathrm{f}}^2}\rho\Pi_{22} = (1.1215)^2\pi\rho\sum_{j=1}^{10}\frac{d_j}{(1+\rho)^j} \tag{23}$$

is now introduced. The coefficients d_j are given in Table 1. This function has the following limits:

$$\lim_{\rho\to 0}\chi(\rho) \to 0 \quad \lim_{\rho\to\infty}\chi(\rho) \to 1 \tag{24}$$

The first two terms in eqn (17) are also expressed as energy per unit area in terms of the solution to the thin film problem. Differentiation with respect to $\boldsymbol{e}$ gives the following expression for the generalized stresses,

Table 1
Coefficients for $\chi(\rho)$

j	d_j
1	0.25256
2	0.27079
3	−0.49814
4	8.62962
5	−51.24655
6	180.96305
7	−374.29813
8	449.59474
9	−286.51016
10	73.84223

$$\boldsymbol{\sigma} = \frac{b}{d}\boldsymbol{C}_{\rm hf}(\boldsymbol{e}-\boldsymbol{a}_{\rm hf}\Delta T)+\left(1-\frac{b}{d}\right)\boldsymbol{C}_{\rm s}(\boldsymbol{e}-\boldsymbol{a}_{\rm s}\Delta T)-\frac{b}{d}t\frac{1-\nu_{\rm f}^2}{E_{\rm f}}\chi(\rho)\boldsymbol{Q}_{\rm f}^{\rm T}\boldsymbol{Q}_{\rm f}(\boldsymbol{e}-\boldsymbol{a}_{\rm f}\Delta T) \tag{25}$$

where $\boldsymbol{C}_{\rm hf}$ and $\boldsymbol{a}_{\rm hf}$ are the homogenized stiffness matrix and thermal expansion vector, respectively, for a substrate with a continuous thin film, and $\boldsymbol{C}_{\rm s}$ and $\boldsymbol{a}_{\rm s}$ are the stiffness matrix and thermal expansion vector, respectively, for a bare substrate. The properties for the substrate with a continuous thin film are calculated using standard laminate theory. The first order approximation of $\boldsymbol{C}_{\rm hf}$ and $\boldsymbol{a}_{\rm hf}$, in terms of $\delta = t/h$, for an isotropic homogeneous film on an isotropic substrate are:

$$\boldsymbol{C}_{\rm hf} = \frac{E_{\rm s}h}{1-\nu_{\rm s}^2}\begin{bmatrix}\boldsymbol{P}_{\rm s} & 0\\ 0 & \frac{1}{3}\left(\frac{h}{2}\right)^2\boldsymbol{P}_{\rm s}\end{bmatrix}+\delta\frac{E_{\rm f}h}{1-\nu_{\rm f}^2}\begin{bmatrix}\boldsymbol{P}_{\rm f} & \frac{h}{2}\boldsymbol{P}_{\rm f}\\ \frac{h}{2}\boldsymbol{P}_{\rm f} & \left(\frac{h}{2}\right)^2\boldsymbol{P}_{\rm f}\end{bmatrix} = \boldsymbol{C}_{\rm s}+\delta\boldsymbol{C}_{\rm f} \tag{26}$$

$$\boldsymbol{a}_{\rm hf}^{\rm T} = [a_{\rm s}\ \ a_{\rm s}\ \ 0\ \ 0\ \ 0\ \ 0]+\beta_{\rm film}\begin{bmatrix}\frac{h}{6} & \frac{h}{6} & 0 & 1 & 1 & 0\end{bmatrix} \tag{27}$$

where

$$\boldsymbol{P}_{\rm s} = \begin{bmatrix}1 & \nu_{\rm s} & 0\\ \nu_{\rm s} & 1 & 0\\ 0 & 0 & \frac{1-\nu_{\rm s}}{2}\end{bmatrix},\quad \boldsymbol{P}_{\rm f} = \begin{bmatrix}1 & \nu_{\rm f} & 0\\ \nu_{\rm f} & 1 & 0\\ 0 & 0 & \frac{1-\nu_{\rm f}}{2}\end{bmatrix} \tag{28}$$

and the coefficient of thermal curvature for a continuous thin film is given by

$$\beta_{\rm film} = \delta\left(\frac{6}{h}\right)\left(\frac{E_{\rm f}}{E_{\rm s}}\right)\frac{(1-\nu_{\rm s})}{(1-\nu_{\rm f})}(\alpha_{\rm f}-\alpha_{\rm s}) \tag{29}$$

The zeroth order terms are in both cases the terms corresponding to the bare substrate.

Identification of eqn (25) with eqn (6) gives the following first order approximation of the effective stiffness matrix for the substrate/line system:

$$\boldsymbol{C} = \boldsymbol{C}_{\rm s}+\delta\left(\frac{b}{d}\right)(\boldsymbol{C}_{\rm f}-h\rho\Pi_{22}\boldsymbol{Q}_{\rm f}^{\rm T}\boldsymbol{Q}_{\rm f}) \tag{30}$$

and the following first order approximation of the effective thermal expansion vectors.

$$\boldsymbol{\beta} = \left(\frac{b}{d}\right)\beta_{\rm film}\left(\begin{bmatrix}1\\1\\0\end{bmatrix}-\frac{\chi(\rho)}{1-\nu_{\rm s}}\begin{bmatrix}\nu_{\rm f}-\nu_{\rm s}\\ 1-\nu_{\rm s}\nu_{\rm f}\\ 0\end{bmatrix}\right),\quad \boldsymbol{\alpha} = \begin{bmatrix}\alpha_{\rm s}\\ \alpha_{\rm s}\\ 0\end{bmatrix}+\frac{h}{6}\boldsymbol{\beta}. \tag{31}$$

Note that the only parameters that affect the ratio between the coefficients of thermal

curvature are the Poisson ratios of the lines and substrate, respectively, and the line aspect ratio ρ.

The volume-averaged stresses in the lines can now be computed by considering the first order approximations given by eqns (30) and (31). The bending moments $\boldsymbol{M}$ required to keep the substrate flat after a temperature change ΔT can, to a first order in δ, be expressed as:

$$\boldsymbol{M} = -\frac{E_s h^3}{12(1-v_s^2)}\boldsymbol{P}_s\boldsymbol{\beta}\Delta T. \tag{32}$$

This moment is related to the volume averaged stresses $\langle\sigma_{\alpha\beta}\rangle$ in the lines as:

$$\boldsymbol{M} = \delta\left(\frac{b}{d}\right)\frac{h^2}{2}\begin{bmatrix}\langle\sigma_{11}\rangle\\ \langle\sigma_{22}\rangle\\ \langle\sigma_{12}\rangle\end{bmatrix}. \tag{33}$$

A first order approximation for the volume averaged stresses in the lines expressed in terms of substrate curvatures is obtained from eqns (3), (32) and (33).

$$\begin{bmatrix}\langle\sigma_{11}\rangle\\ \langle\sigma_{22}\rangle\\ \langle\sigma_{12}\rangle\end{bmatrix} = -\frac{E_s}{6(1-v_s^2)}\frac{h^2}{t}\left(\frac{d}{b}\right)\boldsymbol{P}_s\boldsymbol{\kappa}. \tag{34}$$

This result is in accordance with Yeo et al. (1995). Note that, for known substrate curvatures, no knowledge of the material properties of the lines is required. Inserting the analytical expression for the curvature, eqns (3) and (31) into eqn (34), now gives

$$\begin{bmatrix}\langle\sigma_{11}\rangle\\ \langle\sigma_{22}\rangle\\ \langle\sigma_{12}\rangle\end{bmatrix} = \sigma_{\text{film}}\begin{bmatrix}1-\chi(\rho)v_f\\ 1-\chi(\rho)\\ 0\end{bmatrix} \tag{35}$$

where

$$\sigma_{\text{film}} = -\frac{E_s}{6(1-v_s)}\frac{h^2}{t}\beta_{\text{film}}\Delta T = \frac{\alpha_s-\alpha_f}{1-v_f}E_f\Delta T \tag{36}$$

Equations (35) and (36) imply that this approximation may be considered as an extension of the approximate stress/curvature relation for a continuous thin film deposit derived by Stoney (1909). The advantage of the Stoney formula is that if the curvature is known, the film stresses can be determined without knowledge of the film properties. Equations (35) and (36) make it possible to predict line stresses from measurements of thin film curvature measurements in the pre-etched state. Note that the only parameters that affect the ratio between the volume-averaged stresses is the Poisson ratio of the lines (which may be obtained from bulk properties since the Poisson ratio is essentially unaffected by film or line thickness) and the line aspect ratio. With the limit properties of $\chi(\rho)$ stated in eqn (24), it is easy to show that the

curvature relations given by eqns (3) and (31) as well as the volume-averaged stresses in eqn (35) fulfil the analytical limits presented by Shen et al. (1996).

$$\lim_{\rho\to 0}\frac{\kappa_{11}}{\kappa_{\text{film}}}\to\frac{b}{d}\quad \lim_{\rho\to 0}\frac{\kappa_{22}}{\kappa_{\text{film}}}\to\frac{b}{d}\quad \lim_{\rho\to\infty}\frac{\kappa_{22}}{\kappa_{11}}\to -\nu_{\text{s}} \tag{37}$$

$$\lim_{\rho\to 0}\langle\sigma_{11}\rangle,\langle\sigma_{22}\rangle\to\sigma_{\text{film}}\quad \lim_{\rho\to\infty}\langle\sigma_{22}\rangle\to 0\quad \lim_{\rho\to\infty}\frac{\langle\sigma_{11}\rangle}{\sigma_{\text{film}}}\to 1-\nu_{\text{f}} \tag{38}$$

It is now possible to find the following limits as well:

$$\lim_{\rho\to\infty}\frac{\kappa_{11}}{\kappa_{\text{film}}}\to\frac{b}{d}\frac{(1-\nu_{\text{f}})}{(1-\nu_{\text{s}})}\quad \lim_{\rho\to\infty}\frac{\kappa_{22}}{\kappa_{\text{film}}}\to -\nu_{\text{s}}\frac{b}{d}\frac{(1-\nu_{\text{f}})}{(1-\nu_{\text{s}})}. \tag{39}$$

3. Finite element formulation

In order to verify the accuracy and reliability of the present theory, a number of geometries and two different material combinations were investigated and compared with finite element calculations. The material combinations considered are: a silicon substrate with patterned silicon oxide lines (SiO_2–Si), a silicon substrate with copper lines (Cu–Si) and a silicon substrate with aluminum lines (Al–Si). The thermoelastic properties for Si and SiO_2 have been retrieved from Shen et al. (1996). The material data for Al and Cu were taken from Gouldstone et al. (1998). The material properties listed in Table 2 are values applicable in the range 20–450°C. For Al (1 wt.% Cu) alloys, the elastic and thermal properties are assumed to be essentially the same as those of pure aluminum. Note that the thermal expansion coefficient for Al is the largest followed by that for Cu, Si and SiO_2. The elastic moduli are the largest for Si, and the smallest for SiO_2 and Al.

In the finite element calculations, the general purpose finite element program ABAQUS (1997) was used. One half of a periodic cell was modeled by one layer of twenty-noded isoparametric brick elements in the x_2–x_3 plane. Periodic boundary conditions consistent with the effective strains $\boldsymbol{e}$ according to eqn (5) were applied to the FE-model in combination with a temperature change ΔT. The thermoelastic properties were then basically computed by use of eqn (6). Details of the technique

Table 2
Material properties valid in the temperature range 20–450°C

	E [Gpa]	ν	α [10^{-6} K^{-1}]
Substrate Si	166.1	0.262	3.0065
Lines Al	61.1	0.33	26.58
Lines SiO_2	71.4	0.16	0.6383
Lines Cu	120.4	0.35	18.4

used to extract homogenized properties may be found in Adolfsson and Gudmundson (1997). The number of elements used in the computations varied between 1236 and 3223 depending on the geometry. In order to judge the accuracy of the finite element results, a coarser mesh with an approximately doubled characteristic element length was also used. The difference between the dimensionless thermal curvature coefficients and dimensionless volume averaged stresses retrieved from the two simulations was in all cases smaller than 1.5%. The present finite element formulation gives results identical to the generalized plane strain model presented by Shen et al. (1996). The geometrical parameters held constant in the FE simulations are:

$$d = 3\mu m, \quad \delta = 0.001 \tag{40}$$

The ratio d/b and the aspect ratio ρ were varied in the simulations.

4. Comparison of theory with finite element and experimental results

4.1. Si substrate with Al lines

In Fig. 3 the dimensionless thermal curvature coefficients parallel and perpendicular to the lines are shown as functions of the aspect ratio t/b for different d/b ratios. It is observed from the finite element results that the dimensionless curvatures show some dependence on d/b, especially across the lines, and when t/b is smaller than one. The dependence on d/b is almost completely non-existent for the cases when $d/b = 2.1$ and

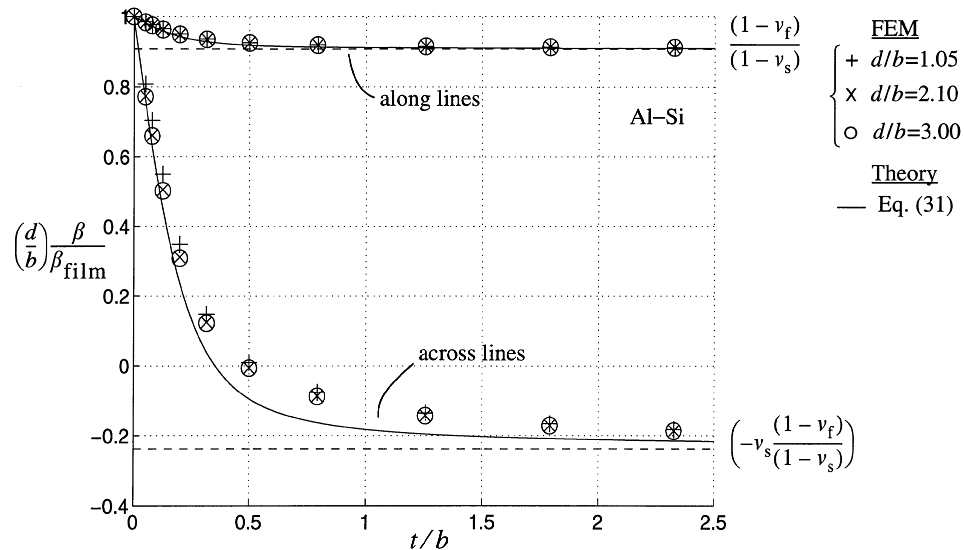

Fig. 3. Si wafer with Al lines. Dimensionless curvatures versus aspect ratio t/b for $d/b = 1.05$, 2.1 and 3.0. Solid lines represent analytical results, the symbols represent FE results and the dashed lines denote asymptotic limits.

3.0. The analytical model, given by eqn (31), for the dimensionless curvature along the lines shows very good accuracy compared to the finite element solution. The accuracy of the analytical model across the lines, is not as good when the aspect ratio is about one half, but the magnitude of the dimensionless curvature is also small in that range. It is also seen that the analytical solution underestimates the aspect ratio ρ corresponding to zero curvature across the lines. This effect is mainly due to the difference in elastic modulus between the lines and the substrate, since the analytical model is based on stress intensity factors for an infinite row of equidistant cracks in a semi-infinite homogeneous isotropic medium.

In Fig. 4 the dimensionless volume-averaged stresses parallel and perpendicular to the lines are shown as functions of the aspect ratio t/b for different d/b ratios. The dependence on d/b is very limited here as well: it is only obvious for the crack case $d/b = 1.05$. Experimental results obtained by Yeo et al. (1995) for Al (1 wt.% Cu) lines on a Si substrate are also included. These experimental data are based on curvature measurements, on the basis of which the stresses were extracted using eqn (34). The agreement between the FE and analytical predictions is very good along the lines. However, the experimental data for large aspect ratios along the lines depart markedly from these predictions. As noted by Yeo et al. (1995) the validity of the experimental results is ostensibly questionable for line aspect ratios greater than unity, as a consequence of a number of effects including creep and plasticity. It is observed that the theoretical volume-averaged stress across the line tends to zero as the aspect ratio increases. This is reasonable since the surfaces of the lines are stress-free and the shape of the line in this limiting case implies plane stress. It is observed that when the

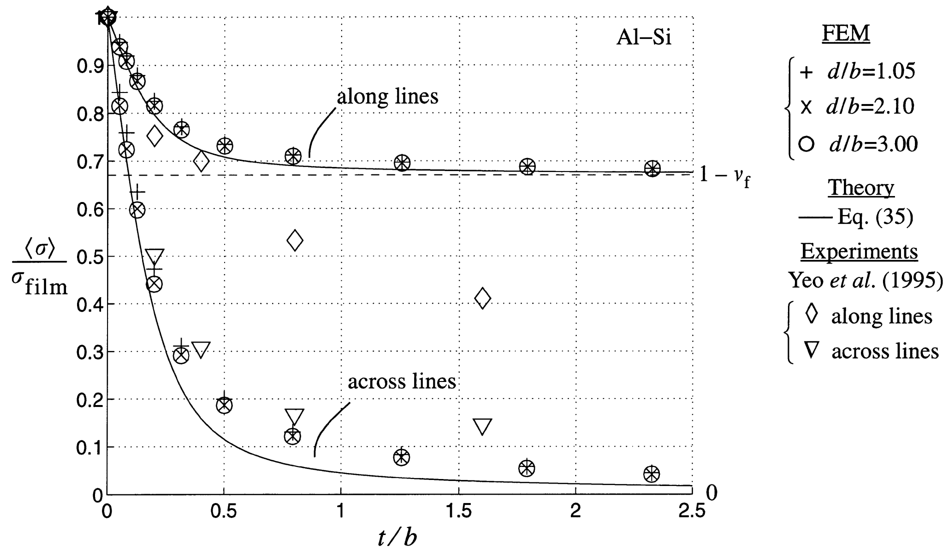

Fig. 4. Si wafer with Al or Al(Cu) lines. Dimensionless volume-averaged stresses versus aspect ratio t/b. Solid lines represent analytical results, the symbols +, x, o represent FE results for $d/b = 1.05$, 2.1 and 3.0. Experiments by Yeo et al. (1995) are indicated by $\diamond$ and $\triangledown$. Dashed lines denote asymptotic limits.

aspect ratio is larger than approximately one, the changes in curvature and the volume-averaged stress are small and the limit expressions in eqns (38) and (39) may give sufficient accuracy.

4.2. Si substrate with Cu lines

The elastic modulus of Cu is much closer to the elastic modulus of Si than that of Al and SiO_2 (Table 2). Since the analytical model is based on stress intensity factors for an infinite row of equidistant cracks in a semi-infinite homogeneous isotropic medium, predictions for copper lines should give better agreement with the FE results for line aspect ratios around one half. In Fig. 5, a comparison between the analytical, eqn (35), and FE predictions for volume averaged line-stresses are presented. It is observed that, as expected, the agreement is better and the deviation for lines with $d/b = 1.05$ is smaller than that for $d/b = 2.1$, 3.0.

Note that even for the case of $d/b = 1.05$, which is expected to conform to the surface crack analogue closely, there can be a noticeable difference between the analytical and finite element results (e.g. Fig. 4). This difference is mainly due to the mismatch in the elastic modulus between the lines and the substrate. The deviation between theory and numerical simulations, however, is reduced when the elastic mismatch is lower, as in the case of Cu lines on Si substrate.

4.3. Si substrate with SiO_2 lines

In Fig. 6, the present analytical results are compared to FE results and experiments presented by Shen et al. (1996). The general trends regarding differences between

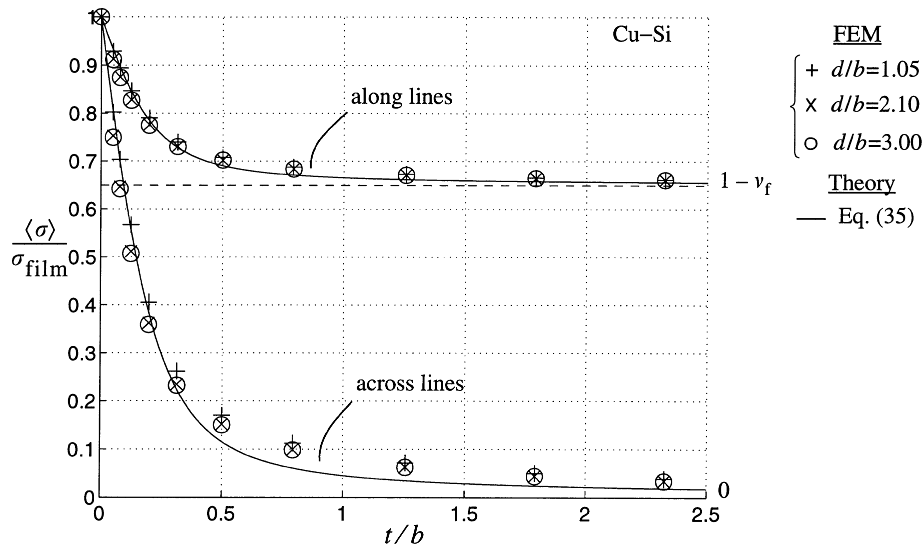

Fig. 5. Si wafer with Cu lines. Dimensionless volume averaged stresses versus aspect ratio t/b for $d/b = 1.05$, 2.1 and 3.0. Solid lines represent analytical results, the symbols represent FE results and the dashed lines asymptotic limits.

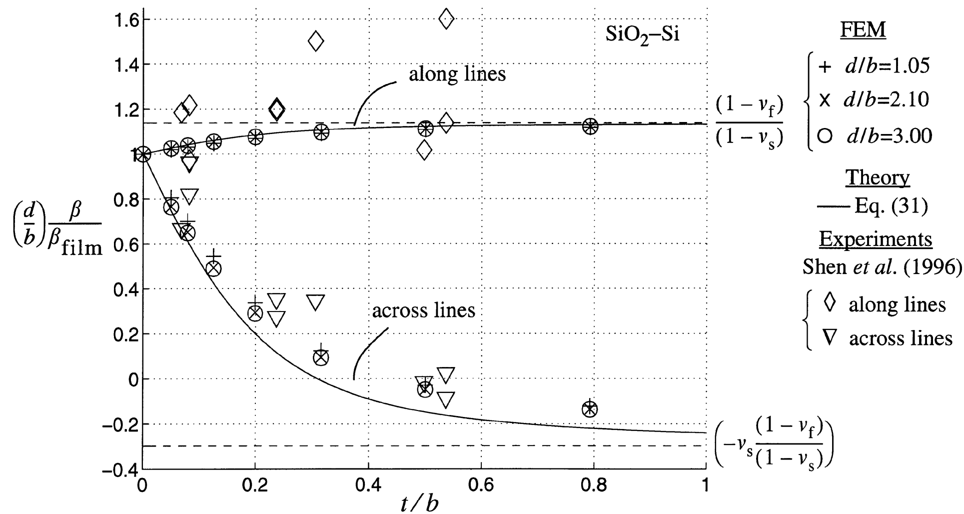

Fig. 6. Si wafer with SiO_2 lines. Dimensionless curvatures versus aspect ratio t/b. Solid lines represent analytical results, the symbols +, x, o, represent FE results for $d/b = 1.05$, 2.1 and 3.0. Experiments by Shen et al. (1996) are indicated by $\diamond$ and $\triangledown$. Dashed lines show asymptotic limits.

finite element simulations and analytical results are the same as in Fig. 3. The reason for the dimensionless curvature along the lines becoming larger than unity is that the Poisson ratio for the substrate is greater than that of the SiO_2 lines. Note that the experimental line curvature is divided by the corresponding experimental film curvature. It is seen that the experimental results deviate from the finite element results and the analytical result. It is however observed that the general behavior is the same. Some pairs of experimental results seem to be biased upwards in the figure. It is noted by Shen et al. (1996) that the accuracy in the measurements are smaller for small film thicknesses and for curvatures normal to the lines. In Fig. 7 the ratio between the dimensionless curvature across the lines and the dimensionless curvature along the lines are shown as a function of the aspect ratio t/b. It is seen that the match between theoretical and experimental results is much better here. It is also seen that the experimental results are closer to the finite element results than to the analytical solution. The dimensionless volume-averaged stresses are shown in Fig. 8. It is observed that the decrease in volume-averaged stress with t/b along the lines is much less pronounced than for aluminum and copper lines.

5. Conclusions

This paper reports analytic expressions which, to a reasonable accuracy, predict the thermoelastic properties and average line stresses for a periodic array of unpassivated thin lines on substrates. The expressions, which are given in eqns (31) and (35), are easy to apply for quick estimates of curvatures and volume-averaged line stresses.

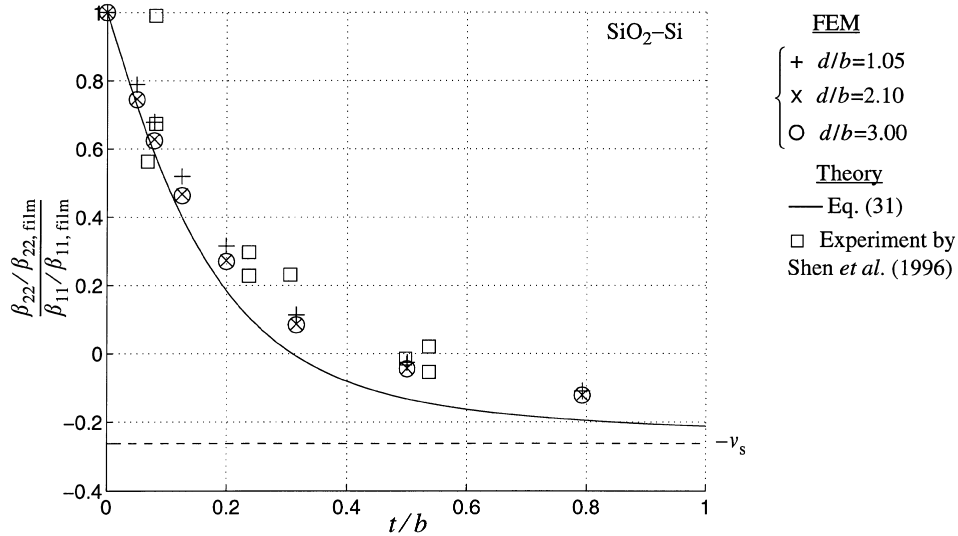

Fig. 7. Si wafer with SiO_2 lines. Ratio between dimensionless curvatures versus aspect ratio t/b. Solid lines represent analytical results, the symbols +, x, o represent FE results for $d/b = 1.05, 2.1$ and 3.0. Experiments by Shen et al. (1996) are indicated by □. Dashed lines show asymptotic limits.

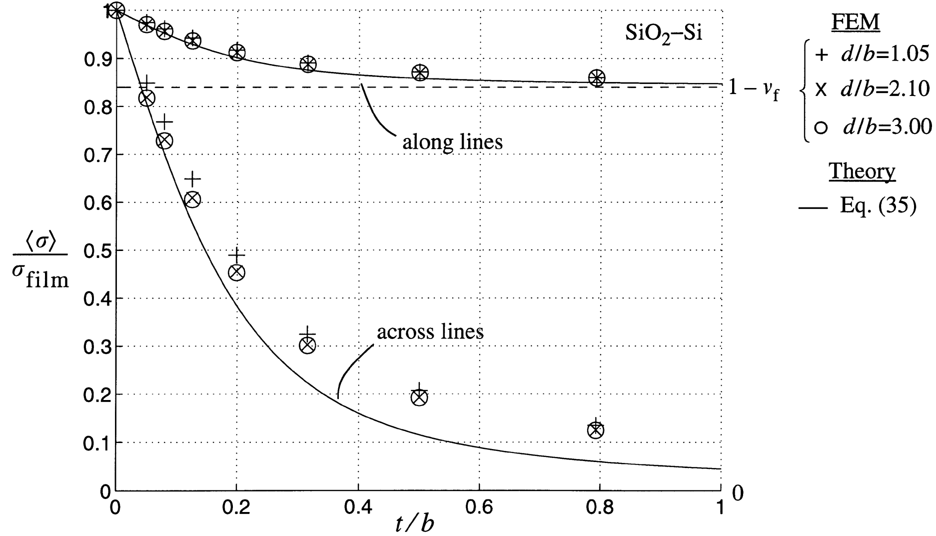

Fig. 8. Si wafer with SiO_2 lines. Dimensionless volume averaged stresses versus aspect ratio t/b for $d/b = 1.05, 2.1$ and 3.0. Solid lines represent analytical results, the symbols represent FE results and dashed lines denote asymptotic limits.

A noteworthy outcome of the present theory is that it enables the determination of stresses and curvatures in the line/substrate system from a knowledge of the film stress, for any arbitrary geometry. This implies that even though the model does not include the effect of plasticity, it can be applied for the case of line etching when the curvature and stress in the blanket-film case are known, since etching of the film into lines is essentially an elastic unloading situation as shown by Gouldstone et al. (1998). Equation (35) may be interpreted as a generalization of the well known Stoney formula for a thin film. The analytical expressions given in eqns (31) and (35) converge to known theoretical limits at the extreme cases of $t/b \rightarrow 0$ and $t/b \rightarrow \infty$. Considering the experimental difficulties typically encountered in the measurement of small curvatures, especially those perpendicular to the lines, the present analytical predictions are judged to be sufficiently accurate for the entire range of line geometries. It has been observed that for an aspect ratio larger than ~ 1, the asymptotic expressions for the thermal curvature coefficients, eqns (37) and (39), and for the volume-averaged stresses, eqn (38) are expected to yield sufficient accuracy.

Acknowledgements

The authors acknowledge Dr Mårten Olsson for valuable discussions during the course of this work. SS is grateful to the Swedish Research Council for Engineering Sciences (TFR) for the award of the Swedish National Chair in Mechanical Engineering at the Royal Institute of Technology during 1997–1998 which facilitated this research.

References

ABAQUS, 1997. Version 5.6, General Purpose Finite Element Program. Hibbit, Karlsson and Sorensen, Inc., Pawtucket, RI, USA.

Adolfsson, E., Gudmundson, P., 1997. Thermoelastic properties in combined bending and extension of thin composite laminates with transverse matrix cracks. Int. J. Solids Structures 34, 2035–2060.

Aleck, B.J., 1949. Thermal stresses in a rectangular plate clamped along an edge. J. Appl. Mech. 16, 118–122.

Besser, P.R., Marieb, T.M., Lee, J., Flinn, P.A., Bravman, J., 1996. Measurement and interpretation of strain relaxation in passivated Al–0.5% Cu lines. J. Mater. Res. 11, 184–193.

Blech, I.A., Levi, A.A., 1981. Comments on Aleck's stress distribution in clamped plates. J. Appl. Mech. 48, 442–445.

Blech, I.A., Meieran, E.S., 1967. Enhanced X-ray diffraction from substrate crystals containing discontinuous surface films. J. Appl. Phys. 38, 2913–2919.

Gouldstone, A., Shen, Y.-L., Suresh, S., Thompson, C.V., 1998. Evolution of stresses in passivated and unpassivated metal interconnects. J. Mater. Res., in press.

Gudmundson, P., Zang, W., 1993. An analytic model for the thermoelastic properties of composite laminates containing transverse matrix cracks. Int. J. Solids and Structures 30, 3211–3230.

Hu, S.M., 1979. Film-edge-induced stress in substrates. J. Appl. Phys. 50, 4661–4666.

Isomae, S., 1981. Stress distributions in silicon crystal substrates with thin films. J. Appl. Phys. 52, 2782–2791.

Jones, R.E., Basehore, M.L., 1987. Stress analysis of encapsulated fine-line aluminum interconnect. Appl. Phys. Lett. 50, 725–727.

Korhonen, M.A., Black, R.D., Li, C.-Y., 1991. Stress relaxation of passivated aluminum line metallizations on silicon substrates. J. Appl. Phys. 69, 1748–1755.

Moske, M.A., Ho, P.S., Mikalsen, D.J., Coumo, J.J., Rosenberg, R., 1993. Measurement of thermal stress and stress relaxation in confined metal lines: I—stresses during thermal cycling. J. Appl. Phys. 74, 1716–1724.

Sauter, A.I., Nix, W.D., 1992. Thermal stresses in aluminum lines bounded to substrates. IEEE Trans. Compon. Hybrids. Manuf. Technol. 15, 594–600.

Shen, Y.-L., Suresh, S., Blech, I.A., 1996. Stresses, curvatures and shape changes arising from patterned lines on silicon wafers. J. Appl. Phys. 80, 1388–1398.

Stoney, G.G., 1909. The tension of metallic films deposited by electrolysis. Proc. R. Soc. Lond. A82, 172–175.

Yeo, I.-S., Ho, P.S., Anderson, S.G.H., 1995. Characteristics of thermal stresses in Al(Cu) fine lines: I—unpassivated line structures. J. Appl. Phys. 78, 945–952.